REFERENCES

[1] J. J. Wysocki, "Lithium-doped radiation-resistant silicon solar cells," *IEEE Trans. Nuclear Science*, vol. NS-13, pp. 168–173, December 1966.

[2] P. H. Fang and Y. M. Liu, "Temperature dependence of radiation damage in silicon," *Phys. Lett.*, vol. 20, pp. 344–346, March 1, 1966.

[3] J. R. Carter, R. G. Downing, and H. Flicker, "Charged particle radiation damage in semiconductors—XII: Effects of high energy electrons in silicon and silicon solar cells," Contract NAS 5-3805, May 25, 1966.

[4] R. V. Tauke, "Thermal annealing of irradiated *n*-on-*p* silicon solar cells," U. S. Naval Research Lab., Washington, D. C., NRL Progress Rept., pp. 1–6, December 1965.

[5] P. H. Fang, "Annealing of radiation induced defects in silicon," *Phys. Lett.*, vol. 20, pp. 343–344, March 1, 1966.

[6] ——, "Thermal annealing of radiation damage in solar cells," NASA Rept. X-713-65-468, November 1965.

[7] R. L. Statler and B. J. Faraday, "Thermal annealing of silicon solar cells irradiated by high-energy electrons," *Bull. Am. Phys. Soc.*, vol. 12, p. 205, February 1967.

[8] R. J. Lambert, "Automatic computation and plotting of spectral response data," U. S. Naval Research Lab., Washington, D. C., NRL Progress Rept., pp. 7–13, February 1964.

[9] ——, "Instrumentation for the direct measurement of outer space short circuit current of solar cells," *Rev. Sci. Instr.*, vol. 36, pp. 1713–1715, December 1965.

[10] W. Rosenzweig, "Diffusion length measurements by means of ionizing radiation," *Bell Sys. Tech. J.*, vol. 41, pp. 1573–1588, September 1962.

[11] R. L. Statler, "Radiation damage in silicon solar cells from 4.6 MeV proton bombardment," U. S. Naval Research Lab., Washington, D. C., NRL Rept. 6333, November 15, 1965.

[12] J. J. Loferski and J. J. Wysocki, "Spectral response of photovoltaic cells," *RCA Rev.*, vol. 22, pp. 38–55, March 1961.

[13] B. R. Gossick, "Disordered regions in semiconductors bombarded by fast neutrons," *J. Appl. Phys.*, vol. 30, pp. 1214–1218, August 1959.

Infrared Heterodyne Detection

M. C. TEICH, MEMBER, IEEE

Abstract—Heterodyne experiments have been performed in the middle infrared region of the electromagnetic spectrum using the CO_2 laser as a radiation source. Theoretically optimum operation has been achieved at kHz heterodyne frequencies using photoconductive Ge:Cu detectors operated at 4°K, and at kHz and MHz frequencies using $Pb_{1-x}Sn_xSe$ photovoltaic detectors at 77°K. In accordance with the theory, the minimum detectable power observed is a factor of $2/\eta$ greater than the theoretically perfect quantum counter, $h\nu\Delta f$. The coefficient $2/\eta$ varies from 5 to 25 for the detectors investigated in this study. A comparison is made between photoconductive and photodiode detectors for heterodyne use in the infrared, and it is concluded that both are useful.

Heterodyne detection at 10.6 μm is expected to be useful for communications applications, infrared radar, and heterodyne spectroscopy. It has particular significance because of the high radiation power available from the CO_2 laser, and because of the 8 to 14 μm atmospheric window.

I. INTRODUCTION

THE USE of heterodyning as a coherent detection method in the radiowave, microwave, and optical[1]–[6] regions of the electromagnetic spectrum is well known. It is the purpose of this paper to show that optimum heterodyne performance may be attained well into the infrared. Experiments performed with several different detector configurations and materials, at the CO_2 laser wavelength (10.6 μm), will be discussed.

Coherent detection differs in several significant respects from direct detection, or simple photon counting. The con-

figuration for a generalized heterodyne receiver is shown in Fig. 1. Its operation is based on the square-law response of the photodetector to the incident radiation electric field. As a result, two electromagnetic waves of different frequencies (ω_1 and ω_2) mix at the photodevice to produce a signal at the difference frequency $\omega_1 - \omega_2$. When one of these beams is strong (it may be locally produced and is then called the local oscillator or LO beam), the sensitivity for the process is considerably greater than in the straight detection or video case because of the high conversion gain between power at the input and at the difference frequency.[2] In addition to this high conversion gain, the heterodyne detector exhibits both strong directivity and frequency selectivity. The frequency selectivity of the coherent detection process, in turn, permits the noise bandwidth to be reduced to a very small value. It is also observed that the heterodyne detector is linear in that the detector output power is proportional to the input signal radiation power.

At optical and infrared frequencies, the heterodyne detector acts, in effect, as both an antenna and a receiver,[7] and requires careful alignment between the LO and signal beams in order to maintain a constant phase over the surface of the photodetector. As a result, the use of coherent detection in a communication system is limited by the atmospheric distortion of the wavefront, which imposes a restriction on the maximum achievable signal-to-noise ratio.[8] Heterodyne detection is therefore most useful for detecting weak signals which are coherent with a locally produced source. It is a relatively insensitive detector for thermal radiation,[7] although it should be pointed out that it is
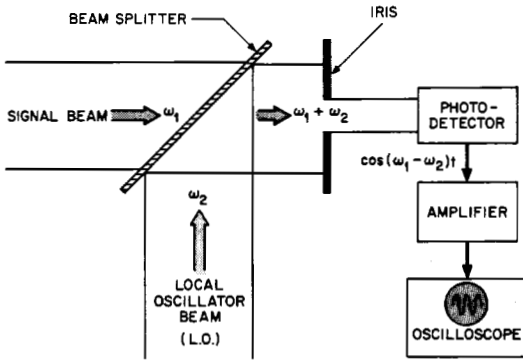
Fig. 1. The generalized infrared or optical heterodyne receiver.

capable of furnishing information about the frequency spectrum.[6]

In the case where both the signal and the LO derive from the same source (such as in the experiments described in this paper), the heterodyne signal can provide information about the velocity of a target through the Doppler shift.[1] Heterodyne detection is also useful for heterodyne spectroscopy[11],[9] and in the study of physical processes occurring in materials. Use of the technique has already been made in the design of a laser Doppler velocimeter, which measures localized flow velocities in gases and liquids.[10],[11]

Coherent detection experiments have been previously reported in the visible and the near infrared using photoemissive devices,[5],[12] photodiodes,[2],[13] and photoconductors.[5],[14],[15] The use of an InAs diode has permitted heterodyne measurements to be extended to 3.5 μm.[16] In the submillimeter region, an improvement in sensitivity with heterodyne operation[17],[18] has been demonstrated for InSb, pyroelectric, and Golay cell detectors.

The measurements reported here have been performed at 10.6 μm in the middle infrared region. It is the availability of the high radiation power from the CO_2 laser coupled with the 8 to 14 μm atmospheric window which makes sensitive detection at 10.6 μm important for systems use. Furthermore, it is at these longer wavelengths that the higher sensitivity available from coherent detection is particularly valuable, since it enables the user to discriminate against various noise sources including the blackbody radiation from objects at room temperature, which is appreciable at 10.6 μm. In the experiments reported below, we have observed a minimum detectable radiation power which is within a factor of 5 of the theoretical quantum limit, $h\nu\Delta f$. (Here, $h\nu$ is the photon energy and Δf is the receiver bandwidth.)

Because the experimental setup employed in these experiments detects the scattered radiation from a diffusely reflecting moving surface, it is, in effect, a miniature prototype CO_2 laser radar. A full-scale CO_2 laser radar based on a similar experimental configuration has been recently set up and successfully operated on targets as far as two miles from the transmitter by Bostick.[19]

---

[1] This is still possible if the LO and signal beams arise from different, but frequency locked, lasers.[3],[6]

II. THEORY

A parameter which is of interest in evaluating the usefulness of a receiving technique is the signal-to-noise ratio. In this section, we discuss the operation of an infrared (optical) heterodyne receiver and calculate the expected signal-to-noise ratio at the output of the detector.

Consider two parallel electromagnetic waves of frequencies ω_1 and ω_2 impinging normally on the photodetector of an infrared heterodyne receiver[3]-[5] (see Fig. 1). The total electric field vector E_t is given by

$$E_t = E_1 \cos \omega_1 t + E_2 \cos \omega_2 t \qquad (1)$$

where E_1 and E_2 are the amplitudes of the individual incident waves. Assuming that E_1 and E_2 have the same polarization, the response r from the detector is proportional to the intensity of the radiation or to the square of the electric field

$$r \propto E_t^2 = E_1^2 \cos^2 \omega_1 t + E_2^2 \cos^2 \omega_2 t$$
$$+ E_1 E_2 \cos(\omega_1 - \omega_2)t + E_1 E_2 \cos(\omega_1 + \omega_2)t. \qquad (2)$$

Because the detector cannot follow the instantaneous intensity at infrared frequencies, it will respond to the average value of the first, second, and fourth terms in (2) above. These average values are $E_1^2/2$, $E_2^2/2$, and zero, respectively. However, it is assumed that the detector has a sufficiently high frequency response to follow the signal at the difference frequency $\omega_1 - \omega_2$. Thus, the response of the detector to the two incident waves is given by

$$r = \beta \left[\frac{E_1^2}{2} + \frac{E_2^2}{2} + E_1 E_2 \cos(\omega_1 - \omega_2)t \right] = r_{dc} + r_{IF} \qquad (3)$$

where β is a proportionality constant containing the detector quantum efficiency.

If we confine measurement of the signal to a bandpass about the difference or heterodyne frequency (also called the intermediate frequency or IF), then it follows that

$$r_{IF} = \beta \cdot E_1 E_2 \cos(\omega_1 - \omega_2)t. \qquad (4)$$

But, since $r_{dc} = (\beta/2)(E_1^2 + E_2^2)$, the detector response may be written in terms of its dc component:

$$r = \left[1 + \frac{2E_1 E_2 \cos(\omega_1 - \omega_2)t}{E_1^2 + E_2^2} \right] r_{dc}. \qquad (5)$$

For a very strong LO beam, $E_2 \gg E_1$, and it follows that

$$r_{IF} = 2 \frac{E_1}{E_2} r_{dc} \cos \omega_{IF} t. \qquad (6)$$

The mean-square photodetector response is then given by

$$\langle r_{IF}^2 \rangle = 2 \frac{P_1}{P_2} r_{dc}^2, \qquad (7)$$

where P_1 and P_2 are the radiation powers in the signal beam and the LO beam, respectively.

If we now consider the noise response r_n in the detector as arising from shot noise,[20],[21] which is the case for the

photoemitter and the ideal reverse-biased photodiode, then the mean-square noise response is given by the well-known shot-noise formula

$$\langle r_n^2 \rangle = 2er_{dc}\Delta f. \tag{8}$$

Hence, the signal-to-noise ratio, $(S/N)_{power}$, may be written

$$(S/N)_{power} = \frac{\langle r_{IF}^2 \rangle}{\langle r_n^2 \rangle} = \frac{P_1}{e\Delta f} \left(\frac{r_{dc}}{P_2} \right). \tag{9}$$

However, since r_{dc} arises from the comparatively large LO, it is related to the LO beam power P_2 by the quantum efficiency η

$$r_{dc} = \frac{\eta e}{h\nu} P_2. \tag{10}$$

Thus, the result for the signal-to-noise ratio becomes[20],[21]

$$(S/N)_{power} = \eta P_1 / h\nu\Delta f$$

(photoemitter and reverse-biased photodiode).   (11a)

From this relation, it is seen that the value of the signal beam radiation power necessary to achieve a $(S/N)_{power} = 1$ is given by

$$P_s^{min} = \frac{h\nu\Delta f}{\eta}$$

(photoemitter and reverse-biased photodiode).   (11b)

This quantity is defined as the minimum detectable power, and is denoted by P_s^{min}.

If the two radiation beams impinging on the detector are not parallel to within a certain angular tolerance,[7],[22] and do not illuminate the same area, or if the radiation is not normally incident upon the photodetector,[23] then (S/N) and P_s^{min} will differ from the expressions in (11) given above. In the experiments reported in this work, however, the conditions required for the validity of (11) have been satisfied. For a sufficiently large LO power, the theory derived in the form given above has been experimentally verified both for the case of photoemitters,[5] and for back-biased photodiodes.[13],[16] In particular, Hanlon and Jacobs[24] have recently verified (11) in a bandwidth of 1 Hz, using an InAs diode detector.

For the case of a photoconductor, the noise behavior differs from simple shot noise, and the results derived above are not directly applicable. Photoconductor noise is a complicated phenomenon,[25] and depends to a great extent on the nature of the photoconductor.[2] In the limit of large LO powers, however, extrinsic Ge:Cu is expected to display simple generation-recombination (g-r) noise.[26] Since the behavior for simple g-r noise is the same as that for shot noise except for a factor of two,[15],[26]–[28] it may be shown that the signal-to-noise ratio for Ge:Cu has a value just one-half as large as that for a photoemitter or a nonleaky reverse-biased photodiode of the same quantum efficiency.

The same result has also been obtained as a special case[3] of a relation derived by DiDomenico and Anderson[29] for CdSe.

In the photovoltaic cell, on the other hand, the same processes occur as in the reversed-biased photodiode. However, instead of generating a current, a voltage results from the dipole-layer charge since the cell is effectively open-circuited. The detectivity and the real noise equivalent power (RNEP) for both the reverse-biased p-n junction and the photovoltaic detector have recently been discussed by van Vliet,[25] who has shown that the RNEP for the photovoltaic cell is higher than that for the reverse-biased photodiode by a factor of $\sqrt{2}$. It follows that the (electronic) noise power, which is proportional to the square of the RNEP, is a factor of 2 greater for the photovoltaic configuration. Therefore, the signal-to-noise ratio for the photovoltaic device, as for the photoconductor, is just one-half that for the photoemitter or the reverse-biased photodiode. It should be pointed out, however, that the advantage gained in signal-to-noise ratio for reverse-biased photodiode operation can only be realized for detectors having a high reverse-bias dynamic resistance, as will be seen later.

The signal-to-noise ratio and minimum detectable power for the extrinsic photoconductor and for the photovoltaic junction are therefore given by

$$(S/N)_{power} = \eta P_1 / 2h\nu\Delta f \tag{12a}$$

$$P_s^{min} = \left(\frac{2}{\eta} \right) h\nu\Delta f$$

(photoconductor and photovoltaic diode).   (12b)

These devices are a factor of 2 less sensitive than a photoemitter or ideal reverse-biased photojunction of the same quantum efficiency [compare (11)], and a factor of $2/\eta$ less sensitive than the perfect quantum counter. (For the photoconductor, although both the signal and the noise depend on the photoconductor gain G, the ratio may be shown to be independent of this parameter.[14])

The operation of photoconductive Ge:Cu as a heterodyne detector near the theoretical limit given by (12) has been demonstrated earlier by Teich, Keyes, and Kingston.[30] More recently, similar experiments performed on Ge:Hg by Buczek and Picus[31] have also been found to agree closely with the predictions of (12).

In later sections, we discuss in detail the experimental results of heterodyne measurements on photoconductive Ge:Cu and on photovoltaic $Pb_{1-x}Sn_xSe$. In both of these cases, the experimental agreement with the theory outlined in this section is quite good.

III. Experiment

A schematic diagram of the experimental arrangement used for the heterodyne measurements in photoconductive Ge:Cu is shown in Fig. 2. The radiation from a CO_2-N_2-He laser, emitting approximately 10 W at 10.6 μm, was incident on a modified Michelson interferometer. One mirror of the

---

[2] van Vliet[25] has separated photoconductors into four classes, each of which behaves differently: intrinsic, minority trapping model, two-center model, and extrinsic.
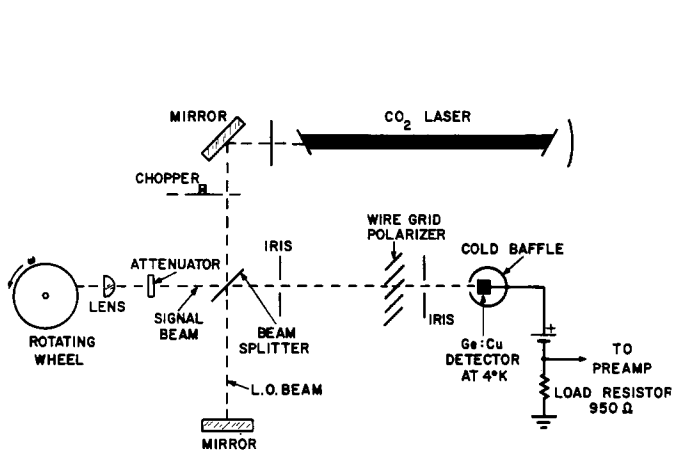
[3] In the absence of trapping.

Fig. 2.   Experimental arrangement for heterodyne measurements with a Ge:Cu detector. The electric field vector lies perpendicular to the plane of the paper.
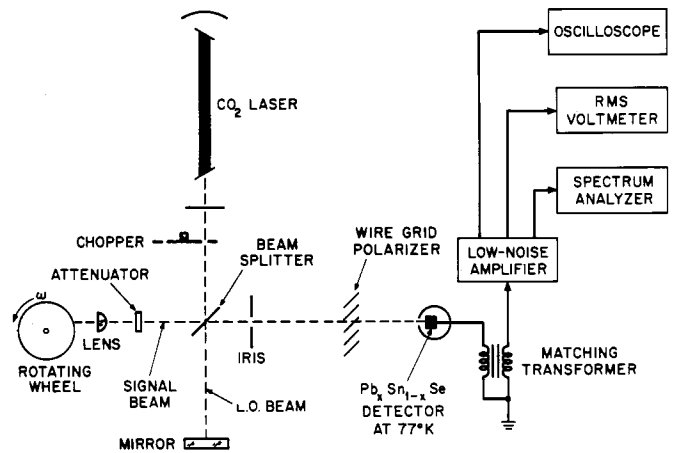
Fig. 3.   Experimental arrangement for measurements with a $Pb_{1-x}Sn_xSe$ detector. The arrangement is similar to that shown in Fig. 2, with the exception of the detector output circuitry.
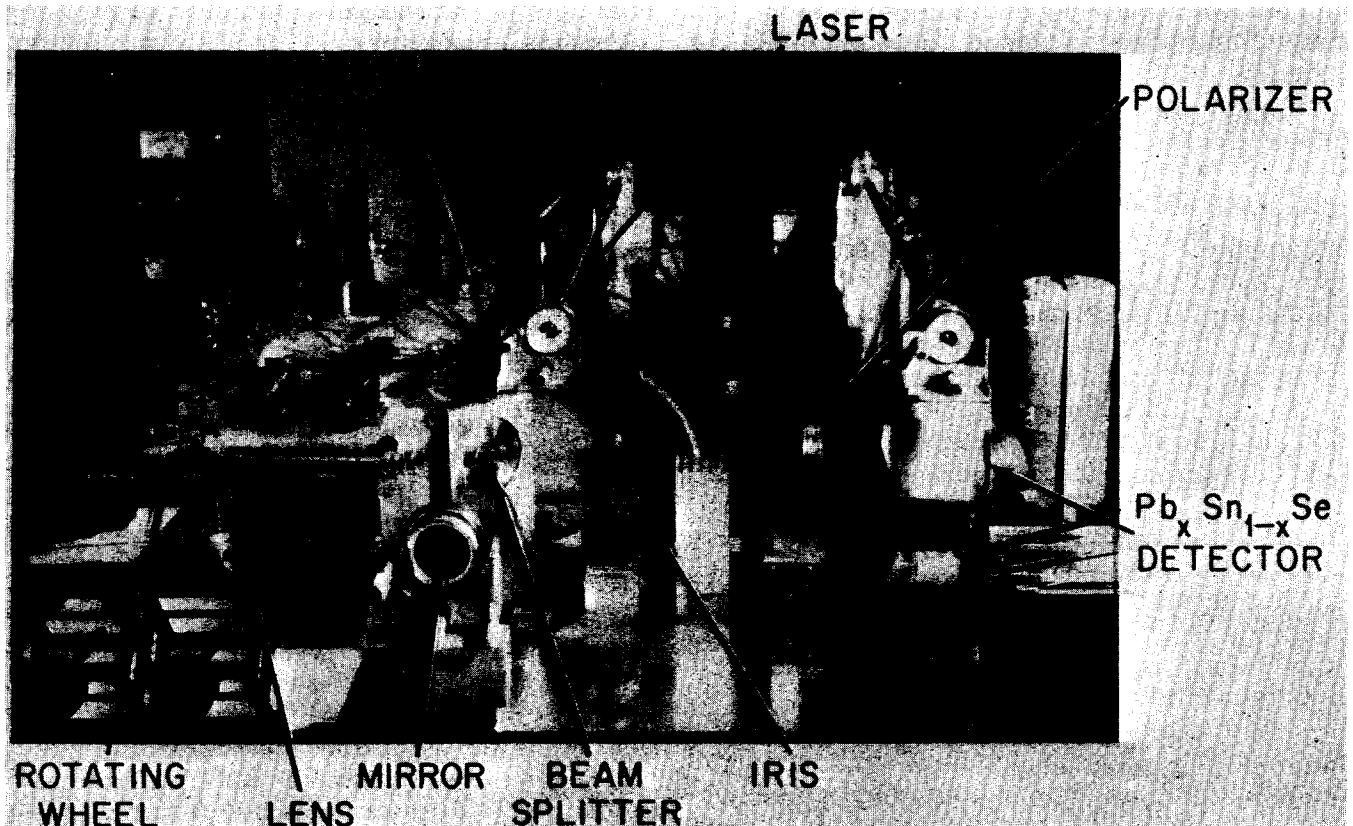

Fig. 4.   Photograph of the heterodyne apparatus.

conventional interferometer was replaced by an off-center rotating aluminum wheel with a roughened surface.

The diffusely scattered radiation from the wheel provided a Doppler-shifted signal which was recombined at the beam-splitter with the unshifted LO radiation reflected from the mirror of the other interferometer leg. Heterodyne detection measurements with scattered radiation at 0.6328 μm have been made previously by Gould et al.[32] and by others.[33] Siegman has calculated the maximum radiation

power to be returned by a random scatterer.[7],[34]

With the exception of the rotating wheel and the chopper, the experimental apparatus was mounted on a granite slab supported by compressed fiberglass blocks. To further minimize the effect of acoustic vibrations, the 1.25-m-long Brewster-window sealed laser tube was set on shock mounts and enclosed in a shield constructed of acoustic tile. The laser was operated well above threshold and on a single line and mode. An uncoated Irtran II flat (of thickness

0.64 cm) served as a beam splitter, and front surface mirrors were of standard aluminum-coated glass.[4]

A 2.54-cm-focal-length Irtran II lens inserted in the signal beam focused the radiation to a single spot on the rim of the rotating wheel. The purpose of the lens was twofold. It served to collect sufficient scattered radiation to permit an incoherent (nonheterodyne) measurement of the scattered signal power at the detector for calibration purposes, and it also insured spatial coherence of the scattered radiation over the receiver aperture. The procedure is analogous to that used to obtain spatially coherent thermal radiation, where the source is focused onto a pinhole aperture stop. This insures that all points on the wavefront emanating from the pinhole arise from the same source point and are therefore correlated. The coherence properties may be deduced from the van Cittert-Zernike theorem.[32],[35]

Irises were used to maintain the angular alignment of the wave fronts of the two beams to within λ/a, the required angular tolerance for optimum photomixing (a is the detector aperture).[7] It should be noted that this angular alignment restriction is twenty times less stringent than in the visible region of the spectrum. A Perkin-Elmer wire-grid polarizer insured that the recombined beams had a common linear polarization. The beams impinged normally on the photodetector. The output from the detector was fed through a controlled-bandwidth, low-noise amplifier to a thermocouple type rms voltmeter. Alternately, the signal was fed simultaneously to an oscilloscope and to a spectrum analyzer.

The experimental setup used for the heterodyne measurements with photovoltaic $Pb_{1-x}Sn_xSe$ is shown in Fig. 3. It is essentially identical to the arrangement for Ge:Cu, with the notable exception of the detector output circuitry. For the high-impedance photoconductor (dark resistance ~ 600 kΩ), a 1-kΩ load resistor is used to convert the photocurrent to a voltage suitable for amplification. For the low-impedance photovoltaic device (~ 1.5 Ω), on the other hand, the voltage is both amplified and transformed in impedance to the standard 50 Ω by the use of a matching transformer. A photograph of the actual experimental equipment used in these measurements is shown in Fig. 4.

IV. RESULTS FOR PHOTOCONDUCTIVE Ge:Cu

The copper-doped germanium detectors used in the heterodyne experiments were made by indiffusion of Cu into high-resistivity n-type germanium host material for a period of 16 hours at 760°C. The samples, which were 2 mm × 2.2 mm × 3 mm in size, were then quenched in air. The resulting copper atom concentration was 6.8×10^{15} cm^{-3}, and the compensation by the original donors was such as to produce a free hole lifetime of about 2×10^{-9} s at 4°K. With a bias voltage of 13.5 V on the detector, its (incoherent) low-power responsivity was found to be 0.2
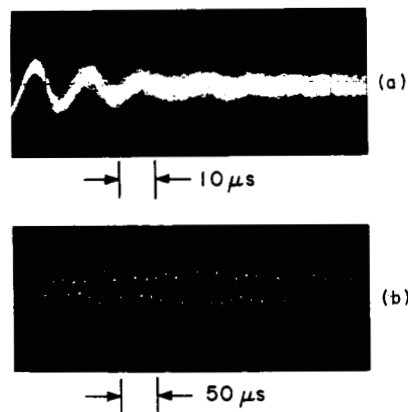

Fig. 5. (a) A multiple-sweep display of the heterodyne signal from a Ge:Cu detector. The loss of definition of the waveform in the third cycle reflects the finite bandwidth of the heterodyne signal. (b) A single-sweep of the signal shown in (a), but with a longer time scale. The modulation of the signal envelope arises from the random nature of the scattering surface.
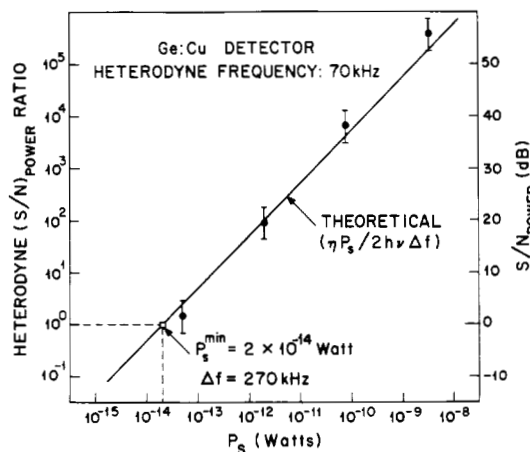

Fig. 6. The data points, obtained from a typical run, represent the observed signal-to-noise ratio of the heterodyne signal in Ge:Cu, $(S/N)_{power}$, for a given signal-beam radiation power (P_s). The theoretical curve, given by the expression $(S/N)_{power} = \eta P_s/2h\nu\Delta f$, is in good agreement with the data. The minimum detectable power P_s^{min} (defined as that signal beam power for which the heterodyne S/N is unity) corresponds, in a 1-Hz bandwidth, to 7×10^{-20} W.

A/W by calibration with a blackbody source of known temperature. The detector was operated near liquid helium temperature.

Fig. 5(a) shows a multiple-sweep display of the heterodyne signal obtained at the detector output with a signal beam radiation power of 1×10^{-8} W. The loss of definition of the waveform in the third cycle reflects the finite bandwidth of the heterodyne signal. Fig. 5(b) shows a single trace of this signal for a longer time scale. The modulation bandwidth is caused by statistical fluctuations of the heterodyne signal arising from the moving diffuse surface of the wheel.

The results of a typical experimental measurement of the heterodyne signal-to-noise ratio for the detector are shown in Fig. 6. The filled circles represent the observed signal-to-noise power ratio data points, $(S/N)_{power}$, as a function of the signal beam radiation power (P_s or P_1). Only noise arising from the presence of the LO beam (which was the dominant contribution to the noise) is considered. Various

---

[4] These mirrors must have high reflectivity to prevent thermal distortion and consequent deformation of the wavefront of the reflected radiation.

values of P_s were obtained by inserting calibrated CaF_2 attenuators in the signal beam, while the unattenuated power was measured by chopping the signal beam in the absence of the LO. As indicated earlier, the presence of the lens facilitated this measurement.

A plot of the theoretically expected result,

$$(S/N)_{power} = \eta P_s/2h\nu\Delta f,$$

is also shown in Fig. 6. Using an estimated quantum efficiency $\eta = 1/2$, it is seen to be in good agreement with the experimental data. Had noise from sources other than the LO been taken into account in computing the S/N, the experimental values would still be within a factor of two of the theoretical curve. Measurements were made with an LO power of 1.5 mW.

With a heterodyne signal centered at about 70 kHz, and an amplifier bandwidth of 270 kHz, the experimentally observed minimum detectable power P_s^{min} (defined as that signal beam power for which the heterodyne S/N is unity) is seen to be 2×10^{-14} W. In a 1-Hz bandwidth, this corresponds to a minimum detectable power of 7×10^{-20} W, which is to be compared with the expected value $(2/\eta)h\nu\Delta f \simeq 7.6 \times 10^{-20}$ W. The experimental measurement is therefore within 6 dB of the theoretically perfect quantum counter, and is in substantial agreement with the expected result for the Ge : Cu detector used in these experiments.

Because the roughness of the wheel (~ 10 μm) is comparable to the radiation wavelength λ, the bandwidth of the noise modulation B should be approximately[30] v/d, where v is the velocity at which the illuminated spot traverses the surface, and d is the diameter of the focused spot on the wheel (~ 50 μm). This follows from the fact that every d/v seconds, a completely new area of the wheel is illuminated, giving rise to scattered radiation which is uncorrelated with that of the previous time interval. The coherence time is therefore $\sim d/v$, and the frequency bandwidth is given by the inverse coherence time. With $v = r\dot{\theta}$ and $d \sim F\lambda/D$, B is given approximately by $r\dot{\theta}D/F\lambda$. Here v is the tangential velocity of the wheel (157 cm/s), $\dot{\theta}$ is its angular velocity (10π s^{-1}), and r its radius (5.05 cm). F represents the focal length of the lens (2.54 cm), while D is the diameter of the radiation beam at the output of the laser (~ 5 mm).

Using these values, we obtain a calculated noise modulation bandwidth $B \sim 30$ kHz, which is comparable with the value obtained from the power-spectral-density trace shown in Fig. 7. A Panoramic model SB-15a ultrasonic spectrum analyzer operated with a trace sweep speed of $\simeq 4$ s^{-1} was used for the observations.[5] The center frequency of 70 kHz is seen to correspond to the period of 14 μs observed in Fig. 5(b). Both traces were obtained directly across the (1-kΩ) photoconductor load resistor.

A discrepancy between the observed values of signal and noise (individually, rather than the ratio) and the values calculated on the basis of the measured responsivity has
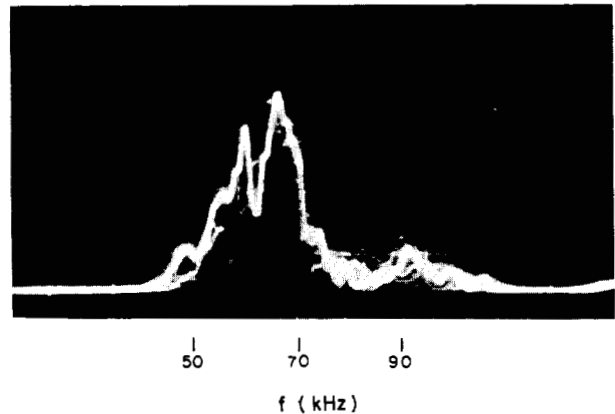

Fig. 7. A typical power-spectral-density trace of the heterodyne signal from Ge : Cu. The trace sweep speed was 4 s^{-1}. The center frequency of 70 kHz corresponds to the period of 14 μs observed in Fig. 5(b).

not been resolved.[30] Experiments have shown, however, that the photoconductor gain does not depend either on the chopping frequency of the incident radiation or on the heterodyne frequency, both possible causes for the disagreement. Other experiments, which have been performed by placing attenuators in various positions in the optical path, indicate that amplification of frequency-shifted (scattered) radiation[36] by the laser is not responsible for the effect.[6] Measurements of the photoconductor gain as a function of the LO power were inconclusive, and it remains possible that this effect has some bearing on the problem.

The results reported in this section differ only slightly from those reported previously for Ge : Cu by Teich, Keyes, and Kingston.[30] Buczek and Picus,[31] in their experiments with Ge : Hg, used two independent CO_2 lasers oscillating at slightly different frequencies. The minimum detectable power which they obtained (referred to a 1-Hz bandwidth) was P_s^{min} (Ge : Hg) $= 1.73 \times 10^{-19}$ W, which is in good agreement with the results obtained by us for Ge : Cu, using a completely different experimental configuration.

V. RESULTS FOR PHOTOVOLTAIC $Pb_{1-x}Sn_xSe$

The $Pb_{1-x}Sn_xSe$ diodes used as heterodyne detectors have been fabricated from Bridgman-grown crystals by Melngailis and by Calawa et al.[37]–[39] The bandgap of these diffused p-n junction devices varies with composition (x) so that the wavelength for peak responsivity may be adjusted by varying x. The devices which we used achieved their maximum responsivity (~ 1 V/W, 77°K) at the CO_2 laser wavelength, and had the composition $Pb_{0.936}Sn_{0.064}Se$. The nature and inversion properties of the conduction and valence bands for these alloys have been discussed in detail both for the diodes[37]–[39] and for single-crystal thin films.[40] The inversion behavior of the bands in $Pb_{1-x}Sn_xSe$ is similar to that observed for $Pb_{1-x}Sn_xTe$.[41] The detectivity of the devices (D^*) was $> 3 \times 10^9$ cm · $s^{-1/2}$ · W^{-1}, and the carrier concentration was $\sim 10^{17}$ cm^{-3}.

---

[5] A smooth, bell-shaped curve may be obtained by integrating and then recording the power spectral density curve.

[6] The author is grateful to A. E. Siegman of Stanford University for discussing this problem with him and suggesting such a possibility.
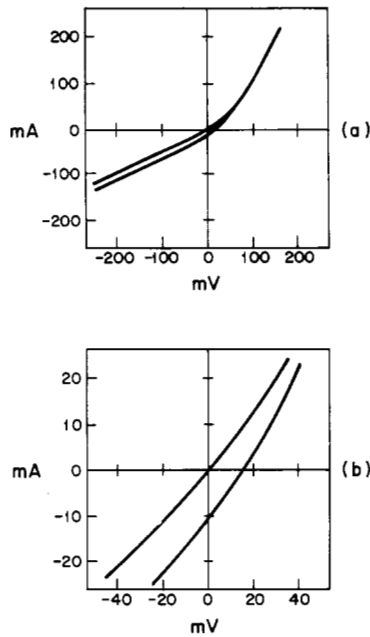
Fig. 8. (a) Current-voltage (I-V) characteristic of the $Pb_{0.936}Sn_{0.064}Se$ diode used in the heterodyne experiments. The upper trace is the dark characteristic while the lower trace is the characteristic with the (18 mW) LO applied. (b) Same characteristic on expanded I and V scales.

Fig. 9. The solid line is the observed signal-to-noise ratio for the heterodyne signal in $Pb_{1-x}Sn_xSe$ as a function of the signal beam radiation power. The heterodyne frequency is 110 kHz and the detection bandwidth is 65 kHz. The theoretical curve, $(S/N)_{power} = \eta P_s/2h\nu\Delta f$, lies within the limit of experimental accuracy.

The diodes had a 1-mm-diameter active area and were operated at 77°K in the photovoltaic mode. The thin n-type layer (~ 10 μm) was exposed to the LO and signal beam radiation. The I-V characteristic of diode no. 37, both in the absence and in the presence of the LO, is shown in Fig. 8. It can be seen from these curves that the zero-current impedance, as well as the reverse impedance, of the detector is $\simeq 1.5$ Ω. This value, which is very low, is essentially independent of the presence of the LO. Using a calibrated thermopile and the I-V characteristic of Fig. 8, the quantum efficiency and responsivity for the device were directly determined to be 8.5 percent and 0.9 V/W, respectively. The efficiency could presumably be further improved by depositing an antireflection coating on the diodes. The numerical values for the quantum efficiency and the responsivity are consistent with those obtained by Melngailis using a different method at much lower radiation powers.

The arrangement used in the heterodyne experiments (see Fig. 3) has been described in detail in Section III. A transformer at the output of the detector transformed its impedance to a level appropriate for matching to the low-noise amplifier. The experimental procedure was identical to that described for measurements on Ge : Cu in Section IV: various values of the signal beam radiation power P_s were obtained by inserting calibrated CaF_2 attenuators in the signal beam. The unattenuated power was determined from the known responsivity of the diode by chopping the signal beam in the absence of the LO, and then using phase-sensitive detection. In all cases, the direct response of the detector was ascertained to depend linearly on the LO radiation power. In calculating the signal-to-noise ratio, only noise arising from the presence of the LO was considered. The noise figure of the amplifier was such that with
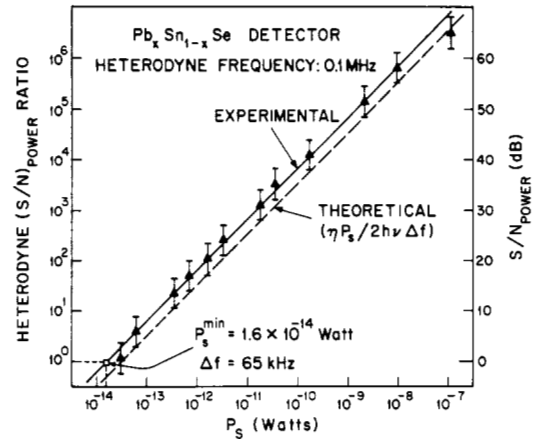
modest LO powers ~ 15 mW, the noise associated with the LO was typically ~ 25 percent of the total noise. It appears that higher LO powers could have been used without any difficulty; however, it would have required a rearrangement of our apparatus to obtain LO powers in excess of 20 mW.

Experiments were performed in two different regions of heterodyne frequency and bandwidth: an IF of 110 kHz with a bandwidth of 65 kHz; and an IF of 2.05 MHz with a bandwidth of 10.0 MHz. They are described in the following paragraphs.

A. Heterodyne Detection at kHz Frequencies

A Princeton Applied Research Model AM-2 input transformer (frequency range 5 kHz to 150 kHz; turns ratio 1 to 100) was used to couple the detector output to the high input-impedance low-noise amplifier (PAR Model CR4-A). Measurements were made with an LO power of 9 mW.

The results of a typical experiment are shown in Fig. 9. The solid line is the observed signal-to-noise power ratio, $(S/N)_{power}$, of the heterodyne signal as a function of the signal beam radiation power P_s. With a heterodyne signal centered at 110 kHz, and a transformer-amplifier bandwidth of 65 kHz, the experimentally observed minimum detectable power P_s^{min} is seen to be 1.6×10^{-14} W. The dashed line in Fig. 9 represents the theoretical result. Using the relation $(S/N)_{power} = \eta P_s/2h\nu\Delta f$, and a quantum efficiency $\eta = 0.085$, it is seen to lie within the limit of experimental accuracy. The observed minimum detectable power corresponds, in a 1-Hz bandwidth, to 2.5×10^{-19} W. Since the experiments were performed using a scattering surface, however, it must be kept in mind that the observation bandwidth for the heterodyne signal must be greater than the noise modulation bandwidth (~ 50 kHz for an IF of 100 kHz).

B. Heterodyne Detection at MHz Frequencies

The behavior of the $Pb_{1-x}Sn_xSe$ heterodyne detectors at MHz frequencies was investigated by rotating the scattering wheel faster. This was accomplished by replacing the 300-r/min synchronous motor driving the scattering wheel
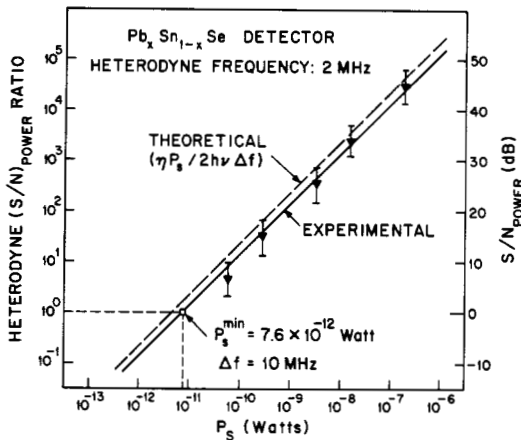
Fig. 10. Signal-to-noise ratio as a function of signal beam radiation power for 2.05 MHz heterodyne signal from $Pb_{1-x}Sn_xSe$. The agreement of theory and experiment, as in Fig. 9, is good.

Fig. 11. (a) A multiple-sweep display of the heterodyne signal in $Pb_{1-x}Sn_xSe$. The loss of definition of the waveform in the fifth cycle reflects the finite bandwidth of the signal. (b) A single sweep of the heretodyne signal shown in (a), but with a longer time scale. This figure is similar to Fig. 5 for Ge:Cu; note the very different time scales, however.

with a 3600-r/min motor. A small matching transformer[7] provided an impedance of approximately 50 Ω at the input of a wide-bandwidth low-noise integrated-circuit amplifier. The effective bandwidth of the transformer-amplifier combination was 10.0 MHz. The LO power was determined from Fig. 8 (and the known responsivity of the detector) to be 18 mW.

The signal-to-noise ratio for the heterodyne signal at 2.05 MHz is shown in Fig. 10. This plot is similar to that of Fig. 9, except for the IF and the bandwidth. The minimum detectable power for this experiment is 7.6×10^{-12} W, which is larger than that of Fig. 9 because of the increased bandwidth. The dashed line, representing the theoretical result, predicts a P_s^{min} of 4.8×10^{-12} W, which is within the experimental bracket. The observed minimum detectable power, extrapolated to a 1-Hz bandwidth, is 7.6×10^{-19} W, which may be compared with the expected value $(2/\eta)h\nu\Delta f \simeq 4.8 \times 10^{-19}$ W.

Fig. 11(a) shows a multiple sweep display at the detector output which is similar to that shown for Ge : Cu in Fig. 5. The loss of definition of the waveform in the fifth cycle reflects the finite bandwidth of the heterodyne signal. Fig. 11(b) shows a single trace of this signal for a longer time scale. Since the noise modulation bandwidth B and the heterodyne frequency are both proportional to the angular velocity of the scattering wheel $\dot\theta$, their ratio is independent of the IF and depends only on geometrical factors. Therefore, Figs. 5 and 11 appear very much alike in spite of their very different time scales.

Heterodyne detection has also been observed in $Pb_{1-x}Sn_xTe$ diodes[37],[42],[43] operated in the photovoltaic mode. The particular alloy composition used had $x=0.17$ ($Pb_{0.83}Sn_{0.17}Te$), which has its peak response at 10.6 μm when operated at 77°K. The detector output voltage was observed to be proportional to the square root of the signal power ($\propto \sqrt{P_s}$), as is expected for heterodyne operation. The responsivity of these preliminary diodes was too
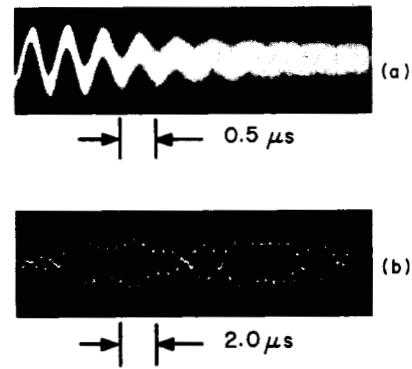
low, however, to observe the noise associated with the LO. This, of course, is necessary for optimum heterodyne detection.

VI. A COMPARISON BETWEEN PHOTOCONDUCTORS AND PHOTODIODES IN THE INFRARED

It has been demonstrated in the previous sections that optimum heterodyne detection has been achieved in the infrared using both photoconductive and photovoltaic detectors. The question of the advantages of each naturally arises.

The signal-to-noise ratio for heterodyne detection was given in Section II, where it was shown that, for equal quantum efficiency, the nonleaky reverse-biased photodiode has a $(S/N)_{power}$ which is superior to that of the photoconductor and the photovoltaic device by a factor of two. Therefore, from the point of view of S/N, it is preferable to operate a (sufficiently high reverse-impedance) diode in a back-biased, rather than in a photovoltaic or photoconductive, configuration. This statement is also valid for direct detection, where the detectivity D^* for reverse-biased operation is augmented by $\sqrt{2}$ over photovoltaic and photoconductive operation.[25] On the other hand, a leaky photodiode characteristic may give rise to adverse effects when operated back-biased, as discussed by Pruett and Petritz.[44]

Aside from the possible improvement in signal-to-noise ratio, another advantage in operating a photodiode in the reverse-biased configuration may be increased frequency response. DiDomenico and Svelto[45] and Lucovsky et al.[13] have shown that the frequency response for a heterodyne photodiode is either transit-time or RC limited. Reverse-biasing increases the diode depletion layer, reducing the capacity of the device and therefore increasing its frequency response. (Reducing the carrier density also will decrease the diode capacity.) However, the $Pb_{1-x}Sn_xSe$ photodiodes which we employed had RC time constants ~1.5 ns (with $R \simeq 1.5$ Ω and $C \simeq 1100$ pF), which was considerably less than the 20-ns response time. (The response time was measured by connecting the diode directly to a

---

[7] Turns ratio 11 to 55, no. 30 wire, on a Ferroxcube Corporation 7F160 cup core. This transformer exhibited a sizeable resonance at about 200 kHz.

properly terminated 50-Ω line, and illuminating it with a 1-ns risetime GaAs injection-laser pulse.) We conclude that these diodes are presently limited by transit time (presumably through the ~ 10-μm n-type layer) to the junction. This transit time could be reduced by decreasing the thickness of the n-type layer without loss of responsivity.

Photovoltaic operation may be preferred in certain cases. For example, with diodes having a low reverse impedance, a reverse voltage could cause undue heating. In photovoltaic operation, the circuitry is simpler,[25] and with low reverse-resistance devices ($< 50 \Omega$), the use of a broadband transformer might be adequate for impedance transformation and a satisfactory amplifier noise figure for frequencies up to ~ 1 GHz.[46]

For the photoconductor with ohmic contacts, the basic frequency response is similar to that of the photodiode, except that it is lifetime or RC limited[14],[45],[47] rather than transit-time limited. Using fast pulse techniques in 2-mm^3 samples of uncompensated and Sb-compensated Ge:Cu ($C \sim 10$ pF), Bridges[48] has recently observed a frequency response of ~ 1 ns, which is quite close to the RC limit for the 50-Ω system which he used. Similar measurements have been made by Buczek and Picus[31] in the several-hundred-MHz region. It should be mentioned that, using proper compensation, Ge:Cu detectors with lifetimes as short as 10^{-12} s have been made at this laboratory. However, it must be kept in mind that when high-frequency response is obtained by matching into a 50-Ω system, the responsivity of the high-impedance photoconductor is considerably reduced.

For optimum heterodyne detection, it is necessary that the LO be sufficiently strong so as to provide the dominant source of noise (to overcome the amplifier noise). A high responsivity is therefore desirable so that the LO radiation power may be kept moderate. Because the photoconductor responsivity is proportional to the photoconductor gain G, which is given by τ/T where τ is the free-carrier lifetime and T is the transit time across the device,[28] it is higher for thin photoconductors. Therefore, a compromise between responsivity and RC frequency response must be made. A discussion of the trade-offs necessary for optimum photoconductor heterodyne operation at high frequencies ($\rightarrow 2$ GHz) has been given by Arams et al.,[49] who have fabricated thin Ge:Cu detectors for this purpose. On the other hand, photodiodes having high reverse impedances should have high responsivity and, since the gain is unity, should in general require less LO than the photoconductor.

Finally, perhaps the most striking characteristic of the $Pb_{1-x}Sn_xSe$ (as well as the $Pb_{1-x}Sn_xTe$ and $Cd_xHg_{1-x}Te$) photodiode detectors is their ability to operate at liquid nitrogen temperatures (77°K). By contrast, Ge:Cu requires near liquid helium temperatures (4°K) while Ge:Hg requires liquid hydrogen temperatures (18°K). The diodes are therefore more convenient to operate and more suitable for field use than are the photoconductors. Nevertheless, the quantum efficiency of the photodiode reported in this work is below that of the photoconductor by a factor of ~ 4, and the minimum detectable power is, therefore, correspondingly higher.

Both photoconductors and photodiodes are seen to be useful for infrared heterodyne detection, the choice of a particular device depending on the desired application.

VII. CONCLUSION

It has been shown that heterodyne techniques, which have been used extensively in the radiowave and microwave regions, and more recently in the optical (visible) portion of the electromagnetic spectrum, are equally as valuable in the infrared.

Coupled with the high power of the CO_2 laser, and the 8 to 14 μm atmospheric window, the optimum-detection heterodyne experiments reported in this work are expected to be significant for communications applications. The operation of the system as an infrared radar has also been demonstrated. The technique might prove useful for infrared heterodyne spectroscopy. It should be pointed out that coherent detection in the infrared is expected to be more sensitive than in the optical region because of the smaller photon energy (the minimum detectable power is proportional to the photon energy).

Further improvements in heterodyne sensitivity may be expected since the quantum efficiency of detectors such as $Pb_{1-x}Sn_xSe$ and $Pb_{1-x}Sn_xTe$, which are presently $\simeq 8$ to 15 percent, show promise of being greater in the future. $Pb_{1-x}Sn_xSe$ detectors have already been operated at dry-ice temperatures ($-78°C$) with a response which is down by only a factor of 20 from the response at 77°K. Furthermore, diodes such as $Cd_xHg_{1-x}Te$[50] (which peak at 10.6 μm with $x = 0.195$) and $Pb_{1-x}Sn_xTe$ have now been fabricated with reverse impedances of $\sim 50 \Omega$ so that impedance matching is less of a problem. With the availability of these higher impedances at the amplifier input, an added advantage is that the noise figure of the amplifier is improved, thus requiring less LO to overcome amplifier noise. Furthermore, if the diode reverse impedance could be raised to a level much greater than that of the load resistance, an additional factor of two could be gained in the signal-to-noise ratio with reverse-biased operation. Thin Ge:Cu photoconductive detectors with high gain as well as short lifetime have been reported by Arams et al.[49] so that heterodyne detection in the GHz range is expected to be possible soon. Therefore, a general relaxation of the few conditions which are still required for efficient infrared heterodyne detection at or near the theoretical limit may be anticipated.

REFERENCES

[1] A. T. Forrester, "Photoelectric mixing as a spectroscopic tool," *J. Opt. Soc. Am.*, vol. 51, pp. 253–259, March 1961.

[2] A. E. Siegman, S. E. Harris, and B. J. McMurtry, "Optical heterodyning and optical demodulation at microwave frequencies," in *Optical Masers*. J. Fox, Ed. New York: Wiley, 1963, pp. 511–527.

[3] S. Jacobs, "The optical heterodyne," *Electronics*, vol. 36, p. 29, July 12, 1963.

[4] M. E. Lasser, "Detection of coherent optical radiation," *IEEE Spectrum*, vol. 3, pp. 73–78, April 1966.

[5] S. Jacobs and P. Rabinowitz, "Optical heterodyning with a CW gaseous laser," in *Quantum Electronics III*, P. Grivet and N. Bloembergen, Eds. New York: Columbia Univ. Press, 1964, pp. 481–487.

[6] L. Mandel, "Heterodyne detection of a weak light beam," *J. Opt. Soc. Am.*, vol. 56, pp. 1200–1206, September 1966.

[7] A. E. Siegman, "The antenna properties of optical heterodyne receivers," *Proc. IEEE*, vol. 54, pp. 1350–1356, October 1966.

[8] D. L. Fried, "Atmospheric modulation noise in an optical heterodyne receiver," *IEEE J. Quantum Electronics*, vol. QE-3, pp. 213–221, June 1967; also "Optical heterodyne detection of an atmospherically distorted wave front," *Proc. IEEE*, vol. 55, pp. 57–67, January 1967.

[9] H. Z. Cummins, N. Knable, and Y. Yeh, "Observation of diffusion broadening of Rayleigh scattered light," *Phys. Rev. Lett.*, vol. 12, pp. 150–153, February 1964.

[10] Y. Yeh and H. Z. Cummins, "Localized fluid flow measurements with an He-Ne laser spectrometer," *Appl. Phys. Lett.*, vol. 4, pp. 176–178, May 1964.

[11] J. W. Foreman, Jr., W. W. George, J. L. Jetton, R. D. Lewis, J. R. Thornton, and H. J. Watson, "Fluid flow measurements with a laser Doppler velocimeter," *IEEE J. Quantum Electronics*, vol. QE-2, pp. 260–266, August 1966.

[12] A. E. Siegman, S. E. Harris, and B. J. McMurtry, "Microwave demodulation of light," in *Quantum Electronics III*, P. Grivet and N. Bloembergen, Eds. New York: Columbia Univ. Press, 1964, pp. 1651–1658.

B. J. McMurtry and A. E. Siegman, "Photomixing experiments with ruby optical maser and traveling wave microwave phototubes," *Appl. Optics*, vol. 1, pp. 51–53, January 1962.

[13] G. Lucovsky, M. E. Lasser, and R. B. Emmons, "Coherent light detection in solid state photodiodes," *Proc. IEEE*, vol. 51, pp. 166–172, January 1963.

G. Lucovsky, R. B. Emmons, B. Harned, and J. K. Powers, "Detection of coherent light by heterodyne techniques using solid state photodiodes," in *Quantum Electronics III*, P. Grivet and N. Bloembergen, Eds. New York: Columbia Univ. Press, 1964, pp. 1731–1738.

[14] M. DiDomenico, Jr., R. H. Pantell, O. Svelto, and J. N. Weaver, "Optical frequency mixing in bulk semiconductors," *Appl. Phys. Lett.*, vol. 1, pp. 77–79, December 1962.

R. H. Pantell, M. DiDomenico, Jr., O. Svelto, and J. N. Weaver, "Theory of optical mixing in semiconductors," in *Quantum Electronics III*, P. Grivet and N. Bloembergen, Eds. New York: Columbia Univ. Press, 1964, pp. 1811–1818.

G. Lucovsky, R. F. Schwartz, and R. B. Emmons, "Photoelectric mixing of coherent light in bulk photoconductors," *Proc. IEEE (Correspondence)*, vol. 51, pp. 613–614, April 1963.

[15] P. D. Coleman, R. C. Eden, and J. N. Weaver, "Mixing and detection of coherent light in a bulk photoconductor," *IEEE Trans. Electron Devices*, vol. ED-11, pp. 488–497, November 1964.

[16] F. E. Goodwin and M. E. Pedinoff, "Application of CCl_4 and $CCl_2:CCl_2$ ultrasonic modulators to infrared optical heterodyne experiments," *Appl. Phys. Lett.*, vol. 8, pp. 60–61, February 1966.

[17] E. H. Putley, "The use of an InSb detector as a mixer at 1 mm," *Proc. IEEE (Correspondence)*, vol. 54, pp. 1096–1098, August 1966.

[18] H. A. Gebbie, N. W. B. Stone, E. H. Putley, and N. Shaw, "Heterodyne detection of sub-millimetre radiation," *Nature*, vol. 214, pp. 165–166, April 1967.

[19] H. A. Bostick, "A carbon dioxide laser radar system," *IEEE J. Quantum Electronics*, vol. QE-3, p. 232, June 1967.

[20] B. M. Oliver, "Signal-to-noise ratios in photoelectric mixing," *Proc. IRE (Correspondence)*, vol. 49, pp. 1960–1961, December 1961.

[21] H. A. Haus, C. H. Townes, and B. M. Oliver, "Comments on 'Noise in photoelectric mixing,'" *Proc. IRE (Correspondence)*, vol. 50, pp. 1544–1546, June 1962.

[22] V. J. Corcoran, "Directional characteristics in optical heterodyne detection processes," *J. Appl. Phys.*, vol. 36, pp. 1819–1825, June 1965.

[23] A. J. Bahr, "The effect of polarization selectivity on optical mixing in photoelectric surfaces," *Proc. IEEE (Correspondence)*, vol. 53, p. 513, May 1965.

[24] J. Hanlon and S. F. Jacobs, "Narrowband optical heterodyne detection," *IEEE J. Quantum Electronics*, vol. QE-3, p. 242, June 1967.

[25] K. M. van Vliet, "Noise limitations in solid state photodetectors," *Appl. Optics*, vol. 6, pp. 1145–1169, July 1967.

[26] H. Levinstein, "Extrinsic detectors," *Appl. Optics*, vol. 4, pp. 639–647, June 1965.

[27] R. C. Jones, "Noise in radiation detectors," *Proc. IRE*, vol. 47, pp. 1841–1846, September 1959.

[28] A. van der Ziel, *Fluctuation Phenomena in Semi-Conductors*. New York: Academic Press, 1959, pp. 22–45 and 65–82.

[29] M. DiDomenico, Jr., and L. K. Anderson, "Signal-to-noise performance of CdSe bulk photoconductive detectors," Bell Telephone Labs., Murray Hill, N. J., unpublished memo.

[30] M. C. Teich, R. J. Keyes, and R. H. Kingston, "Optimum heterodyne detection at 10.6 μm in photoconductive Ge:Cu," *Appl. Phys. Lett.*, vol. 9, pp. 357–360, November 1966.

[31] C. J. Buczek and G. S. Picus, "Heterodyne performance of mercury doped germanium," *Appl. Phys. Lett.*, vol. 11, pp. 125–126, August 1967.

G. S. Picus and C. Buczek, "Far infrared laser receiver investigation," Hughes Research Labs., Malibu, Calif., Interim Tech. Rept. 4, Contract AF33(615)-3847; 1967. See also Repts. 1–3.

[32] G. Gould, S. F. Jacobs, J. T. LaTourrette, M. Newstein, and P. Rabinowitz, "Coherent detection of light scattered from a diffusely reflecting surface," *Appl. Optics*, vol. 3, pp. 648–649, May 1964.

[33] R. D. Kroeger, "Motion sensing by optical heterodyne Doppler detection from diffuse surfaces," *Proc. IEEE (Correspondence)*, vol. 53, pp. 211–212, February 1965.

G. A. Massey, "Photomixing with diffusely reflected light," *Appl. Optics*, vol. 4, pp. 781–784, July 1965.

[34] A. E. Siegman, "A maximum-signal theorem for the spatially coherent detection of scattered radiation," *IEEE Trans. Antennas and Propagation*, vol. AP-15, pp. 192–194, January 1967.

[35] M. Born and E. Wolf, *Principles of Optics*. New York: Pergamon, 1959, pp. 505–510.

[36] W. M. Doyle, W. D. Gerber, and M. B. White, "Use of an oscillating laser as a heterodyne receiver preamplifier," *IEEE J. Quantum Electronics*, vol. QE-3, p. 241, June 1966.

[37] I. Melngailis, "Properties of $Pb_{1-x}Sn_xTe$ and $Pb_{1-x}Sn_xSe$ infrared detectors," presented at the IRIS Infrared Detector Specialty Group Meeting, Wright-Patterson AFB, March 1967.

[38] A. R. Calawa, I. Melngailis, T. C. Harman, and J. O. Dimmock, "Photovoltaic response of $Pb_{1-x}Sn_xSe$ diodes," presented at the Solid State Device Research Conf., University of California at Santa Barbara, June 1967.

[39] J. F. Butler, A. R. Calawa, I. Melngailis, T. C. Harman, and J. O. Dimmock, "Laser action and photovoltaic effect in $Pb_{1-y}Sn_ySe$ diodes," *Bull. Am. Phys. Soc.*, vol. 12, p. 384, March 1967.

[40] A. J. Strauss, "Inversion of conduction and valence bands in $Pb_{1-x}Sn_xSe$ alloys," *Phys. Rev.*, vol. 157, pp. 608–611, May 1967.

[41] J. O. Dimmock, I. Melngailis, and A. J. Strauss, "Band structure and laser action in $Pb_xSn_{1-x}Te$," *Phys. Rev. Lett.*, vol. 16, pp. 1193–1196, June 1966.

[42] I. Melngailis and A. R. Calawa, "Photovoltaic effect in $Pb_xSn_{1-x}Te$ diodes," *Appl Phys. Lett.*, vol. 9, pp. 304–306, October 1966.

[43] I. Melngailis, A. R. Calawa, J.F. Butler, T. C. Harman, and J. O. Dimmock, "Photovoltaic effect in $Pb_xSn_{1-x}Te$ diodes," presented at the Internat'l Electron Devices Meeting, Washington D. C., October 1966.

[44] G. R. Pruett and R. L. Petritz, "Detectivity and preamplifier considerations for indium antimonide photovoltaic detectors," *Proc. IRE*, vol. 47, pp. 1524–1529, September 1959.

[45] M. DiDomenico, Jr., and O. Svelto, "Solid state photodetection: A comparison between photodiodes and photoconductors," *Proc. IEEE*, vol. 52, pp. 136–144, February 1964.

[46] C. L. Ruthroff, "Some broad-band transformers," *Proc. IRE*, vol. 47, pp. 1337–1342, August 1959.

[47] O. Svelto, P. D. Coleman, M. DiDomenico, Jr., and R. H. Pantell, "Photoconductive mixing in CdSe single crystals," *J. Appl. Phys.*, vol. 34, pp. 3182–3186, November 1963.

[48] T. Bridges, to be published.

[49] F. Arams, E. Sard, B. Peyton, and F. Pace, "10.6 micron heterodyne detection with gigahertz IF capability," *IEEE J. Quantum Electronics*, vol. QE-3, pp. 241–242, June 1967; also "Infrared 10.6-micron heterodyne detection with gigahertz IF capability," *IEEE J. Quantum Electronics*, vol. QE-3, pp. 484–492, November 1967.

[50] C. Vérié and J. Ayas, "$Cd_xHg_{1-x}Te$ infrared photovoltaic detectors," *Appl. Phys. Lett.*, vol. 10, pp. 241–243, May 1967.
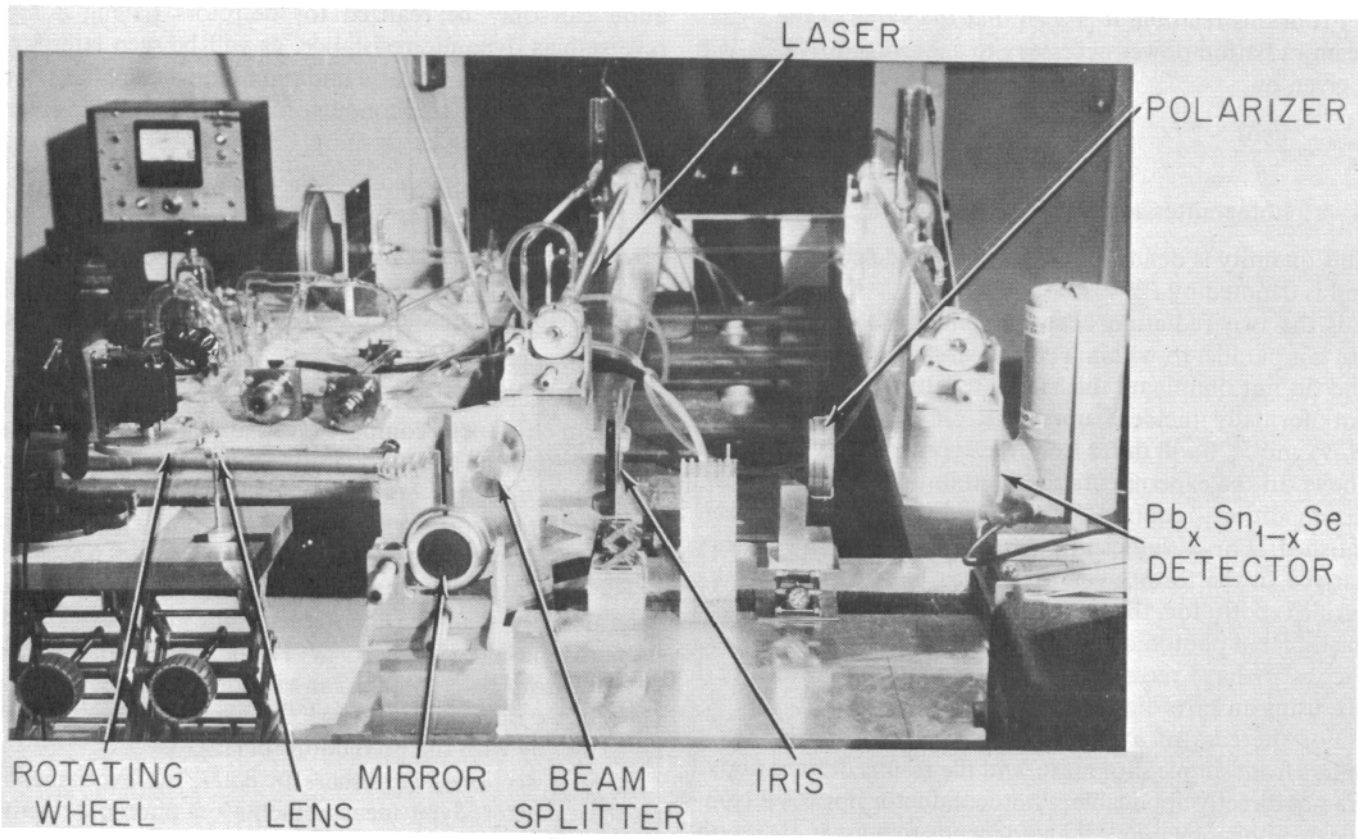
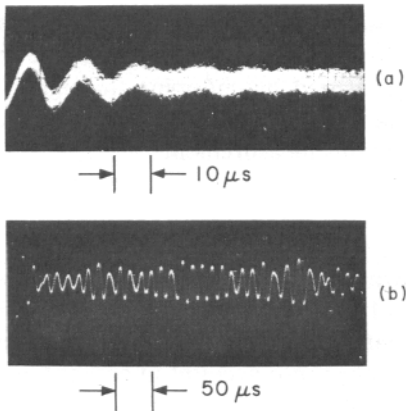Fig. 4. Photograph of the heterodyne apparatus.

Fig. 5. (a) A multiple-sweep display of the heterodyne signal from a Ge:Cu detector. The loss of definition of the waveform in the third cycle reflects the finite bandwidth of the heterodyne signal. (b) A single-sweep of the signal shown in (a), but with a longer time scale. The modulation of the signal envelope arises from the random nature of the scattering surface.
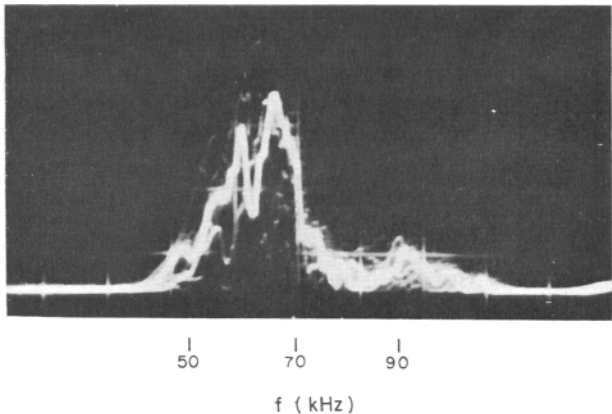
50	70	90

f (kHz)

Fig. 7. A typical power-spectral-density trace of the heterodyne signal from Ge : Cu. The trace sweep speed was 4 s^{-1}. The center frequency of 70 kHz corresponds to the period of 14 μs observed in Fig. 5(b).
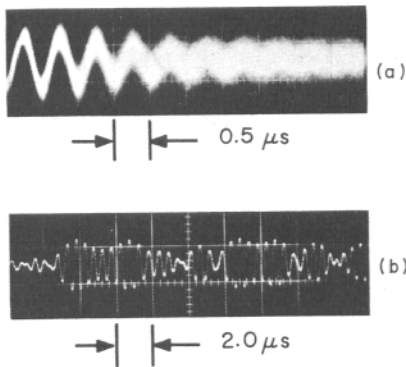
0.5 µs (a)

2.0 µs (b)

Fig. 11. (a) A multiple-sweep display of the heterodyne signal in $Pb_{1-x}Sn_xSe$. The loss of definition of the waveform in the fifth cycle reflects the finite bandwidth of the signal. (b) A single sweep of the heretodyne signal shown in (a), but with a longer time scale. This figure is similar to Fig. 5 for Ge:Cu; note the very different time scales, however.